Allowing the Actual Evapotranspiration Uncertainty in Hydrological Models: Coupling of Interval-Based Water Balance and METRIC Models

Maryam Khodadadi
University of Tehran
Tarokh Maleki Roozbahani
University of Tehran
Mercedeh Taheri
University of Tehran
Fatemeh Ganji
University of Tehran
Mohsen Nasseri (mnasseri@ut.ac.ir)
University of Tehran https://orcid.org/0000-0002-7584-7631

Research Article

Keywords: METRIC, Monthly Water Balance Model, Interval-based Modeling, Uncertainty, GLUE, Evapotranspiration

Posted Date: January 11th, 2022

DOI: https://doi.org/10.21203/rs.3.rs-1110978/v1

Abstract

Against the paramount role of actual evapotranspiration (ET) in hydrological modeling, determining its values is mixed with different sources of uncertainties. In addition, estimation of ET with energy-based methods (e.g., METRIC) leads to different results with various acceptable initial and boundary conditions (such as land use and cold/hot pixels). The aim of the current research is to allow the uncertainty effects of ET as an interval-based input variable in hydrological modeling. The goal is achieved via feeding the uncertainty of computed ET values to the developed Interval-Based Water Balance (IBWB) model in terms of gray values. To this purpose, the comprehensive monthly water balance model (including surface and groundwater modules) has been revised to a new interval-based form. Moreover, the METRIC model has been used 20 times in each month of computational period to calculate the ET patterns with different hot/cold pixels to provide monthly ensemble ET values. For a comprehensive assessment, the selected water balance model has been calibrated with ensemble means of the computed ET with its classical type. The study area is a mountainous sub-basin of the Sefidrood watershed, Ghorveh-Dehgolan basin, with three alluvial aquifers in the North of Iran. Not only the paradigm shift from determinist to interval-based hydrologic structure improved the statistical metrics of the models' responses, but also it decreased the uncertainty of the simulated streamflow and groundwater levels.

1. Introduction

Water resources worldwide are under increasing stress due to various factors such as population growth, land use, and climate change (Murry et al., 2012). In addition, in watersheds under water stress, implementing a comprehensive and accurate assessment is essential to determine sustainable water resources planning and proper management. In this regard, water balance models as a continuous hydrological model along with observational studies are able to evaluate the hydrological behavior of the basin by analyzing the relationships between different types of water storages (soil moisture, groundwater storages, snowpack, and unsaturated moisture storage), inflow, and outflow of water content. However, the performance of water balance models may be limited by different issues, such as the validation of evapotranspiration flux, which is one of the most important components of the hydrological cycle (Corbari et al., 2011, 2015). Therefore, the estimation of actual evapotranspiration (ET) and its accuracy in the modeling are of special importance.

Earth Observation (EO) approach is of key significance in estimating ET due to its appropriate estimation accuracy, economical, and widely spatiotemporal coverage (Zhang et al., 2016; Taghvaeian and Neale, 2011; Schulz et al., 2021). EO-based ET estimation models can vary from entirely empirical methods to physically-based models. Recently in the line of using EO methods in environmental modeling, large-scale evapotranspiration products have been widely used as input (even reference data) to calibrate hydrological models, which are based on combining empirical and physical environmental concepts (Zhang et al., 2009; Vervoort et al., 2014; Lopez et al., 2017; Herman et al., 2018; Kunnath-Poovakka et al., 2018; Jiang et al., 2020, Schoups and Nasseri, 2021).

Energy balance on the land surface is an EO-based solution to apply physical concepts in which remotely sensed information is used widely. The residual method, which estimates ET as the reminder part of the energy balance equation, is one of the most popular methods in the aforementioned methodological fold (e.g., Baeumler et al., 2019; Yin et al., 2020; Al Zayed et al., 2016; Lima et al., 2020; Elkatoury et al., 2020; Çetin and Köksal, 2018; Lian and Huang, 2016; Reyes-González et al., 2017; Taheri et al., 2019, 2021). Based on the research published by Losgedaragh and Rahimzadegan (2018), the Surface Energy Balance Algorithm for Land (SEBAL) (Bastiaanssen et al., 1998 a, b), Mapping Evapotranspiration at high Resolution and with Internalized Calibration (METRIC) (Allen et al., 2007 a, b), and Surface Energy Balance System (SEBS) (Su, 2002) are the most important methods to estimate ET conducted on the energy balance via the residual method.

Based on the METRIC concept, ET has been estimated using boundary conditions named cold and hot pixels. In other words, the amount of ET in the cold pixel is equal to the maximum amount of ET in the region, and in the hot pixel is supposed to be zero, and the ET values in other pixels are interpolated between them. Because the definitions of hot and cold pixels are highly site-specific, so expert judgment in selecting/detecting boundary conditions leads to various responses. This diversity of estimated ET and application of its uncertainties have always been at the highest level of important concerns in developing hydrological models that are connected to this input/proxy information, especially that the estimation of this effective amount is targeted in areas with agricultural development and diversity of manufactured changes.

According to the above-mentioned and as the noble point of the present article, the goal is to hybrid ET values with the water balance model considering its uncertainty. In addition, the effect of the proposed concepts on the simulation of streamflow and groundwater has been evaluated. For this purpose, the comprehensive monthly lumped water balance model (including surface and groundwater modules) has been used. The ET values (interval-based and deterministic) have been simulated using the METRIC model prior to the water balance model. By considering the effects of various alternatives of hot and cold pixels, the uncertain monthly ET (interval values) has been calculated. To use these results, the structure of the comprehensive water balance model has been modified. So that the proposed structure can deterministically simulate the surface and groundwater balances in alluvial aquifers, which is a novel attempt to use interval-based actual ET in a comprehensive water balance model included the effects of agricultural, industrial, and urban harvests.

In the following, after describing the study area, the conceptual comprehensive water balance model and its modification, calculating the ET (deterministic and interval values) have been presented and analyzed. Finally, the results of the modeling procedure and its results have been discussed.

2. Data And Methods

2.1. Study Area

The Sefidrood watershed is one of the most important major watersheds in Iran. Various researches on this watershed were conducted due to its climatic diversity, agriculture, and manufactured developments (e.g., Nosrati et al., 2015; Shayeghi et al., 2020; Taheri et al., 2021; Nasseri et al. 2021). The selected study area is one of the upstream basins in the watershed called Ghorveh-Dehgolan, which finally flows into the Caspian Sea. This mountainous basin is located at latitude 47° 07' 30" and latitude 48° 12' 00"; also, its altitude varies from 1475 to 3150 *m*. The watershed area is about 7302 km^2. According to the

Iran Water Resources Management Company's guidelines regarding water balance modeling, this basin is divided into three main areas: 1) Plain, 2) Highlands Over Looking the Plain (HOLP), and 3) Other Areas (OA). This basin contains three alluvial aquifers located in Chahardooli, Dehgolan, and Ghorveh plains, and each of them has its own HOLP, as well. The area of the aquifers is 781, 169, and 321 km^2, respectively. According to the above classification, the Ghorveh-Dehgolan basin has seven study areas to study the water balance. The connection of the water balance components regarding the topology of the basin is presented in section 3.2. The location of the study areas, the pattern of altitude changes, and the location of hydro-climatological stations are depicted in Fig. 1.

2.2. Ground and Global Gridded Information

Observed variables used in the water balance modules include forcing variables and required variables for the calibration process and evaluation of the results. Forcing data includes precipitation and air temperature. Required data for calibration includes observed monthly streamflow values (recorded at Salamatabad hydrometric station) and monthly groundwater level information over the period of 2000-2001 to 2012-2013. In addition, air temperature and precipitation values have been calculated by Modified Inverse Distance Weighting (MIDW) method (Abedini and Nasseri, 2008) over the watershed. In addition, groundwater levels have been estimated via the Thiessen polygon method. To model evapotranspiration, observations on air temperature (maximum, minimum, and average), wind speed, sunny hours, and relative humidity are required on a monthly time scale. In addition, vegetation products Normalized Difference Vegetation Index (NDVI), Leaf Area Index (LAI), and values of surface temperature and albedo from the MODIS sensor have been used.

2.3. Modeling Procedure

In this section, the numerous components of the modeling procedure are introduced. These items consist of modeling ET using the METRIC algorithm, proposing a comprehensive water balance structure that includes climatological and groundwater modules, and combining the ET estimation model with the presented water balance structure. In fact, by considering the degree of freedom of the METRIC model, an attempt has been made to provide a range of ET of the area. Due to the lack of ground measurements on the ET, the structure of the water balance model has been modified to allow the use of the interval values in its structure. This is the noblest point of the proposed water balance structure. In addition, to evaluate the behavior of the water balance model and its parameters accurately, the uncertainty of the model parameters in the classical (using the results of deterministic ET in the classic-deterministic-water balance model) and the modified models have been evaluated. To assess the models' uncertainties, the Generalized Likelihood Uncertainty Estimation (GLUE) method has been used. In the following, these components are presented in terse statements.

2.3.1. Modeling of Evapotranspiration using METRIC Method

The Mapping Evapotranspiration at high Resolution with Internalized Calibration (METRIC) has been employed to estimate ET (Allen et al., 2007 a, b). According to the METRIC algorithm, ET ($mm.h^{-1}$) is obtained for the satellite overpass time using the residual approach of the surface energy budget equation as follows,

$$ET = 3600\frac{Rn-G-H}{\lambda} \quad (1)$$

where R_n is the net radiation flux ($W.m^{-2}$), G is the soil heat flux ($W.m^{-2}$), H is the sensible heat flux ($W.m^{-2}$), λ is the latent heat of vaporization ($J.kg^{-1}°C^{-1}$), and 3600 is the conversion factor from seconds to hours. The net radiation flux (R_n) is a key term in the energy balance model and is estimated based on the surface radiation budget according to Eq. (2).

$$R_n = (1-\alpha)\,R_{s\downarrow} + R_{l\downarrow} - R_{l\uparrow} \quad (2)$$

where $R_{s\downarrow}$ is the incoming shortwave radiation ($W.m^{-2}$), $R_{l\downarrow}$ is the incoming longwave radiation ($W.m^{-2}$), $R_{l\uparrow}$ is the outgoing longwave radiation ($W.m^{-2}$), and α is the surface albedo. These radiant fluxes have been calculated according to the Eq. (3)-(5),

$$R_{s\downarrow} = G_{sc}.cos\theta.d_r.\mathcal{T}_{sw} \quad (3)$$

$$R_{l\downarrow} = \epsilon_a \sigma T_a^4 \quad (4)$$

$$R_{l\uparrow} = \epsilon_s \sigma T_s^4 \quad (5)$$

Here, G_{sc} is solar constant (1367 $W.m^{-2}$), θ is the solar incidence angle (*rad*), d_r is the inverse squared relative earth-sun distance (m^{-2}), $\mathcal{T}_{sw}$ is the atmospheric transmissivity (*dimensionless*), ϵ_a is the atmospheric thermal emissivity (*dimensionless*), σ is the Stefan-Boltzmann constant (5.67×10^{-8} $W.m^{-2}k^{-4}$), T_a and T_s represent the air and land surface temperature (K), respectively, and ϵ_s is the surface thermal emissivity (*dimensionless*). The relationships presented by Allen et al. (1998), Brutsaert. (1975), and Waters et al. (2002) have been used to estimate $\mathcal{T}_{sw}$, ϵ_a, and ϵ_s, respectively.

The soil heat flux (G) is the conducted heat between the surface and subsurface soil layers due to a temperature difference, and has been calculated based on the R_{net} flux using the following empirical equation (Bastiaanssen, 2000):

$$G = \frac{T_s}{\alpha}(0.0038\alpha + 0.0074\alpha^2)(1-0.98NDVI^4)R_n \quad (6)$$

where *NDVI* is the Normalized Difference Vegetation Index (dimensionless). The sensible heat flux (H) is defined as the rate of heat loss to the air due to the temperature gradient between the surface and atmosphere. It is estimated based on the Bulk Transfer theory and the assumption of the resistance against the heat transfer along with the atmospheric boundary layer. The term H is obtained from Eq. (7):

$$H = (\rho_a \times C_p \times dT)/r_a \quad (7)$$

where ρ_a is the air density at constant pressure ($Kg.m^{-3}$), C_p is the specific heat capacity of air at constant pressure ($J.kg^{-1}.K^{-1}$),r_a is the aerodynamic resistance to heat transport ($s.m^{-1}$), and dT denotes the temperature difference between two specific heights (K) (i.e., 0.1 and 2 *meters*). The term r_a is calculated using Eq. (8):

$$r_a = {}^{1}/_{C_H U} \quad (8)$$

Here, C_H is the heat exchange coefficient (dimensionless), and U is the wind speed at the reference height ($m.s^{-1}$). C_H has been determined using the Monin-Obukhov Similarity Theory (MOST) (Monin and Obukhov, 1959).

METRIC employs an iterative process to update dT and r_a using specific boundary conditions, i.e., cold and pixels. The pixels, which have been used for internal calibration of METRIC, play an effective role in estimating ET with high accuracy. They have been chosen based on the region's characteristics, such as vegetation, land cover, and climate (Allen et al., 2007 a, b). Generally, the cold pixel is selected as a homogenous, wet, and well-irrigated area covered by a full canopy. The surface and near-surface temperatures are similar at this pixel. The hot pixel is defined as a homogenous bare agricultural land, wherein ET is assumed to be zero.

Expert judgment as to the appropriate selection of the pixels can lead to making different choices for anchor pixels, and thus, a diverse range of ET values is provided in each time step. These ET patterns play ensemble roles as a probable pattern of actual ET over the research area. In the current study, the ranges of the collected ensemble ET have been used to stochastically model the water balance, while ET medians are considered to implement a deterministic model. Apparently, the more candidate of hot and cold pixels are selected, the better level of confidence is obtained for the results. The used code of the METRIC method has been developed and evaluated in Taheri et al. (2021).

2.3.2. Water Balance Modeling

In this study, to detect the correct interaction between surface water and groundwater, the combination modules of climatological and groundwater balance models as a comprehensive and integrated water balance model have been used. To this end, the structure of conceptual models developed by Rao and Al-Wagdany (1995) and Kazumba et al. (2008) have been used to model monthly climatological and groundwater balances, respectively. The model uses one layer of soil to store surface moisture and simulates the processes of storing available surface water and interacting with groundwater. In addition, to correct the amount of monthly precipitation over the watershed, a correction factor has been used (de Voss et al., 2010). This coefficient has been added to the parametric degree of freedom of the model, which must be determined during the calibration process. Moreover, the model has been revised using the snow budget proposed by Guo et al. (2005). According to the revision, the separation of precipitation into snow and rain is done by the temperature threshold method (two separate parameters for the snow temperature threshold and rain temperature), and snow melting is calculated by the melting coefficient.

The groundwater balance modeling (based on Kazumba et al., 2008) is conducted via simple and linear reservoirs, and alluvial aquifers are considered as separate tanks and are exchanged with each other through hydraulic conductivity. Due to the role of groundwater in streamflow production, a parameter has been used as Groundwater Threshold (GT) in surface water balance, which has been determined during the calibration process.

Most of the water balance models use empirical or statistical methods to determine ET values (e.g., Thornthwaite and Mather, 1957; Rao and Al-Wagdany, 1995; Xu et al., 1996; Guo et. et al., 2002, 2005; Jazim, 2006). Since the experimental and statistical methods do not consider environmental effects, inaccurate ET values may be estimated. Therefore, in the present study, ET values have been calculated using an energy balance model in the form of the METRIC framework. Based on the proposed methodology, the calculated ET (from the METRIC method) has been extracted from surface water. Its remained part was withdrawn from groundwater resources to wrap up the actual water balance during the modeling period. Fig. 2 shows the conceptual diagram of the proposed comprehensive water balance model, which is based on the Rao surface water and the Kazumba groundwater models. More Details about the model are also provided in Appendix (A).

2.3.3. Combination of Water Balance and METRIC Models

In the present study, two scenarios have been proposed to implement the proposed water balance model by considering the ET values calculated by the METRIC model. In the first scenario, the median ensemble values of ET calculated per month with the requisition to supply it with available water and through penalties in the calibration process are used.

Unlike the first scenario, where the value of ET is assumed to be constant, in the second scenario, it is possible to consider an interval for the amount of ET. In other words, if the median values of ET are not supplied by the available water, its amount can be reduced to a minimum of ET per month so that it is equivalent to the available surface water plus the soil moisture in that month. After revising the interactions of the water balance components, including implementing actual ET, withdrawal from groundwater model, and snow budget, the Interval-Based Water Balance (IBWB) is proposed. In the proposed IBWB model, the ET loss has been provided based on the available water, which is included the sum of snowfall, soil moisture of the surface layer with a delay in each time step, rainfall from which the amount of direct runoff has been deducted, and the calculated returned water (returned water of agricultural farms, industrial or municipal effluents). So, the conceptual components of the proposed IBWB are as same as the determinist comprehensive water balance model, as described before, except the withdrawal from groundwater considering the interval ET values. In the developed IBWB model, the ET band is used instead of the median value. Thus, after obtaining the ET band from the remote sensing data, the model is allowed to oscillate the amount of ET in the interval. Thus, if the available water is sufficient to provide median ET, ET is considered equal to median ET. However, if the available water is less than the median ET, the model is allowed to reduce the ET rate to the lower value of the calculated interval of ET. In addition, it should be noted that the seasonal adjustment

coefficient is considered for the ET band, the value of which is optimized during the calibration process. The minimum evapotranspiration values are considered by seasonal adjustment coefficients (four distinct coefficients for each season) to adjust the values as it is used to adjust for precipitation.

Including the uncertainty of ET based on the proposed method provides a possibility commensurate with the uncertain and complex nature of ET to estimate and apply it in water balance modeling.

2.3.4. Uncertainty Assessment Method

The Generalized Likelihood Uncertainty Estimation (GLUE) technique is a global uncertainty assessment method based on the Monte Carlo sampling-simulation and Equifinality hypothesis that is proposed by Beven and Binley (1992). This method has been used in the uncertainty assessment of various hydrological and environmental models because of its simplicity and effectiveness (Beven and Binley, 2014; Mirzaei et al., 2015). In addition, the GLUE method has been used as a benchmark global uncertainty assessment method in various researches (e.g., Solomatine and Sheresta, 2009; Nasseri et al., 2013, 2014; Wani et al. 2017; Ahmadi and Nasseri, 2020, Yin et al. 2020).

In the current research, the GLUE has been employed to assess the parametric uncertainty of the proposed water balance models, including its determinist and modified interval-based frameworks. The readers are addressed to Mirzaei et al. (2015) for more details and citations of the GLUE method. Although the famous uncertainty assessments using the GLUE method with a single likelihood function are dominated in the literature, multiple criteria GLUE method has been used due to the importance of streamflow and groundwater level in the current research. This method has been used before in Yin et al. (2020), Pang et al. (2019), Xiang et al. (2019), and Smith et al. (2019). The selected likelihood function in the current research is Nash-Sutcliff (NSE) (Nash and Sutcliffe, 1970), which is introduced in the coming section.

2.4. Evaluation and Calibration: Metrics and Methods

In this section, the optimization method, and the implemented statistical indicators that have been used to compare and evaluate the uncertainties and efficiencies of the water balance models, are presented.

2.4.1. Evaluation Metrics

For statistical evaluation of the results and comparing observed and computed streamflow values and groundwater level, Nash-Sutcliff (NSE) (Nash and Sutcliffe, 1970), coefficient of determination (R^2) and Kiling-Gupta Efficiency (KGE) metric (Gupta et al., 2009, Knoben et al. 2019) as similarity statistics and Mean Square Error (MSE) as dissimilarity ones and also TaylorS (Lui et al. 2016) index have been used. The R^2 index varies between zero and one, and higher values indicate a better statistical performance of the calculations versus the observed values. On the other hand, lower values of MSE indicate better model performance in simulation. The numeric range of KGE and TaylorS metrics is from negative infinity to 1, and a value of 1 indicates the highest compatibility between the simulated and observed values. Eq. (9) to (12) show the mathematical formulations of the R^2, KGE, MSE, TaylorS, and NSE, respectively,

$$R^2 = \frac{\left[\sum_{i=1}^{n}\left(X_{Obs}-\bar{X_{Obs}}\right)\times\left(X_{Sim}-\bar{X_{Sim}}\right)^2\right]}{\sqrt{\sum_{i=1}^{n}\left(X_{Obs}-\bar{X_{Obs}}\right)^2\times\sum_{i=1}^{n}\left(X_{Sim}-\bar{X_{Sim}}\right)^2}} \quad (9)$$

$$MSE = \frac{1}{n}\sum_{i=1}^{n}\left(X_{Obs}-X_{Sim}\right)^2 \quad (10)$$

$$KGE = 1-\sqrt{(CC-1)^2+(\sigma-1)^2+(\beta-1)^2} \quad (11)$$

$$TaylorS = \frac{4(1+CORR)}{\left(\sigma+\frac{1}{\sigma}\right)^2\times(1+CORR_0)} \quad (12)$$

$$NSE = 1-\frac{\sum_{i=1}^{n}\left(X_{Obs}-X_{Sim}\right)^2}{\sum_{i=1}^{n}\left(X_{Obs}-\bar{X_{Obs}}\right)^2} \quad (13)$$

In the above, *X* represents the simulated and observed variables, including streamflow and groundwater level. $\bar{X}$ and *CC* represent the mean, correlation coefficient, respectively. σ is the ratio of the mean of the computed to the observed values, βis the ratio of the standard deviation of the computed to the observed values and $CORR_0$is the maximum theoretical correlation (in this study, equal to 1). *Sim* and *Obs* represent simulated and observed values, respectively.

To evaluate the performance of the models' uncertainties, two metrics, Average Relative Interval Length (ARIL) and $\mathrm{P}_{\mathrm{level}}$, presented by Jin et al. (2010), have been used. These statistics are calculated using the upper and lower limits of the confidence levels. ARIL describes the amplitude of the uncertainty bands versus the observed values.$\mathrm{P}_{\mathrm{level}}$ also describes how much of the observed data is grouped by the computed uncertain bands. These metrics are calculated according to the following equations,

$$ARIL = \frac{1}{n}\left(\sum_{t=1}^{n}\frac{UpLi_t-LoLi_t}{Obs_t}\right) \quad (14)$$

$$P_{level} = \frac{NQ_{in}}{n}\times 100 \quad (15)$$

In the above formulas, *UpLi* and *LoLi* are the upper and lower values of the uncertainty bands of the confidence intervals, respectively. *t* is the current time step and *n* is the total number of time steps. The value of NQ_{in} indicates the number of observations covered by the indefinite band. In fact, the lower the ARIL index, the lower the uncertain amplitude of the model results. In addition, in a model with good performance, the value of $\mathrm{P}_{\mathrm{level}}$ index equals to the level of confidence. To simultaneously consider these two indicators, the Normalized Uncertainty Efficiency (NUE) has been used (Nasseri et al. 2013, 2014). NUE is calculated by Eq. (16),

$$NUE = \frac{P_{level}}{\omega \times ARIL} \quad (16)$$

where ω is the scale coefficient (which is assumed to be 1). A high value of NUE means a high proportion of the number of observed values surrounded by high and low limits of uncertainty. Therefore, the model with a higher NUE index is preferred to the other model.

2.4.2. Calibration of the Scenarios

In this study, to optimize the parameters of the IBWB model (Table A1, in Appendix), the Shuffled Complex Evolution (SCE-UA) method has been used (Duan and Gupta, 1992; Chu et al., 2011). This method is a powerful global optimization algorithm and is designed based on the characteristics appropriate to the calibration of conceptual models of the basin simulator. Convergence evaluation of the optimization process has also been done by minimizing the MSE statistics for streamflow values (at the outlet of the watershed) and aquifer levels' values. Due to the simultaneous optimization of the parameters of the surface and underground models, the fitness function has become dimensionless and then has been combined as Eq. (17). Due to the high importance of the output flow, this variable in the objective function has gained more weight through the R^2 between simulated and observed values.

$$\mathrm{Z} = \sqrt[4]{\left(\prod_{\mathrm{i}=1}^{3} \frac{\mathrm{MSE_G}}{\mathrm{var(observation_G)}}\right) \times \left(\frac{\mathrm{MSE_Q}}{\mathrm{var(observation_Q)}}\right)^{\left(1-\mathrm{R_Q^2}\right)}} \quad (17)$$

In Eq. (17), MSE_Q represents the mean square error of streamflow, MSE_G indicates the mean square error of the groundwater level, R^2_Q shows the correlation between the observed and computed values of streamflow, and *i* index counts the number of aquifers in the region.

3. Results

In Fig. 3, the proposed procedure of the current research, including three steps and seven sub-steps, has been depicted. Based on the methodology, the results of the statistical assessment (including similarity and dissimilarity metrics) of the developed water balance models (for the both scenarios) in the calibration and validation periods are presented in Table 1. Moreover, the optimized parameters for the both modelling scenarios are presented in Table A1 (in the supplementary material). According to the results, the groundwater levels of all three aquifers in both scenarios have been well adjusted and, their similarity values in calibration and validation periods are considerable. In the coming sections, the results of the calibration procedure have been presented.

Table 1

Evaluation indexes including R^2, MSE, KGE, and TaylorS for calibration and validation period for each scenario

Scenarios		MSE				R^2			
		Dehgolan aquifer	Ghorveh aquifer	Chahardooli aquifer	Streamflow	Dehgolan aquifer	Ghorveh aquifer	Chahardooli aquifer	Streamflow
Calibration	S_{first}	0.56	0.12	0.20	1.08	0.95	0.96	0.93	0.68
	S_{second}	0.39	0.18	0.17	1.23	0.96	0.94	0.94	0.64
Validation	S_{first}	0.19	0.79	0.16	0.72	0.95	0.96	0.93	0.62
	S_{second}	0.38	0.57	0.07	0.58	0.95	0.94	0.94	0.59
		KGE				TaylorS			
Scenarios		Dehgolan aquifer	Ghorveh aquifer	Chahardooli aquifer	Streamflow	Dehgolan aquifer	Ghorveh aquifer	Chahardooli aquifer	Streamflow
Calibration	S_{first}	0.86	0.96	0.96	0.50	0.99	0.99	0.98	0.74
	S_{second}	0.92	0.97	0.96	0.57	0.99	0.98	0.98	0.73
Validation	S_{first}	0.88	0.65	0.88	0.18	0.99	0.97	0.98	0.78
	S_{second}	0.96	0.65	0.89	0.49	0.99	0.97	0.99	0.76

3.1. Results of the Classic Water Balance Model (Deterministic Model)

As shown in Table 1, the groundwater model is well-calibrated according to the statistical metrics. However, as the similarity and dissimilarity statistics have shown, simulation of streamflow has performed poorly in this scenario. The correlation metrics show that the calculation of groundwater and water fluctuations has a good correlation with the observational data. Moreover, their MSE values show that the simulated groundwater fluctuations are slightly different from the recorded values. On the other hand, the KGE values show that the fluctuations and trends of groundwater are well detected. However, the

streamflow has not been able to fit well with its fluctuations and trends as similar as groundwater level. In addition, the TaylorS index shows that the similarity between the observed and simulated values of groundwater and streamflow are acceptable, but its values are lower in the unit of surface water balance.

3.2. Results of the Interval-Based Water Balance (IBWB)

In the second modelling scenario, there is no need to provide a vector of ET values, and the model can reduce the amount of ET to the lower limit of the interval band of ET to adjust the water balance components. The optimized values of direct runoff coefficient (SRC) coefficients in IBWB are lower than the first scenario, which shows that the model has tried to produce less runoff to improve the amount of produced streamflow. This is also because of the greater amount of water available since less water is taken from the available water to ensure evapotranspiration. The calibrated coefficient of the base-flow generation in IBWB is higher, which is a reason for the greater conformity of the calculated fluctuations of the calculated groundwater and observations. Moreover, the amount of Smax in this scenario is less than the first scenario, which indicates that the model is less inclined to retain water in the soil to increase the available water due to less evapotranspiration in the model.

According to the results, the main advantages of the second scenario are reflected by KGE metrics for both calibration and validation periods, and the preeminence of the simulated streamflow with IBWB is clearly depicted. In the table, the better metrics between the scenarios are underlined. As shown in Table 1, also in this scenario, the groundwater level is well modeled considering various statistical metrics for the same reason as the first scenario. Based on the MSE values for both calibration and validation periods, the results show the same performance on simulation of streamflow, but the second scenario provided better performance than the first ones. Considering the R^2 values, the first scenario provided better results than the IBWB (without any significant advantage), but the water balance results of IBWB are slightly better. The results of TaylorS values for water balance models are very close to each other, but the metrics showed the better performance of the first scenario than the second ones with slight improvements. Generally, the proposed IBWB model has better performance than the first scenario based on Table 1.

3.3. Results of Uncertainty Assessments

In this section, the results of the global and parametric uncertainty assessments of both scenarios (deterministic and IBWB) using the multiple-criterial GLUE have been presented. The used likelihood functions were NSE values between observed and simulated values of streamflow and groundwater level. In addition, these threshold values for streamflow and groundwater levels are set to 0.4 and 0.8, respectively. These threshold values have been selected according to the statistical metrics of the optimized models (presented in Table 1). The confidence level for both surface water and groundwater modules has been set to 95%. In addition, prior distributions for all parameters have been set to the uniform distribution. To infer the uncertainty of the models (parameters and outputs), 5000 accepted parameter sets were collected. After the uncertainty assessment, posterior distributions of the behavioral parameters have been reported in Table A4 (the supplementary materials).

Table 2 shows the statistical indicators of the uncertainty assessment both for the streamflow and groundwater level. According to the results, the ARIL metrics for groundwater level in the second scenario are less than/or equal to the first scenario. However, the values of the metric for streamflow shows a decrease of about 10%, which indicates a decrease in the uncertainty of the model's response. Considering the $\mathrm{P}_{\mathrm{level}}$ values, the uncertainty bands of the groundwater modules in the second scenario group more than 90% of their observations. To present the difference of uncertainty results of the simulated streamflow and groundwater level, their results have been depicted in Fig. 5 to Fig. 8. However, they do not have considerable differences based on the figure. The achieved P_{level} and ARIL of the streamflow in the second scenario are better than the first one. In terms of the NUE metric, the IBWB behaves better than the first water balance model in the simulated streamflow and groundwater level. This advantage has the least and highest effect on the surface and groundwater (Ghorveh aquifer) models, respectively. Due to the good simulations of definite and non-definite groundwater levels, the behavior of the two scenarios is more similar to each other in the groundwater level simulations than in the streamflow simulations. In addition, the NUE value of the simulated streamflow of the second scenario is 23% greater than the first scenario.

Table 2
Uncertanty evaluation indexes in each scenario

Scenario	ARIL				P_{level}				NUE		
	Dehgolan aquifer	Ghorveh aquifer	Chahardooli aquifer	Streamflow	Dehgolan aquifer	Ghorveh aquifer	Chahardooli aquifer	Streamflow	Dehgolan aquifer	Ghorveh aquifer	Chahar aquifer
S_{first}	0.02	0.01	0.01	9.95	98.96	86.46	95.83	51.04	49.4686	94.9292	68.633
S_{second}	0.02	0.01	0.01	8.30	94.79	91.67	91.67	52.08	52.3697	103.1779	70.358

4. Discussion

The model mechanism for producing surface flow in the second scenario has performed better than in the first scenario due to the four statistics. Therefore, it has led to better groundwater evaluation indicators in the second scenario. In evaluating the optimal values of the parameters, the decrease of precipitation adjustment coefficient indicates the tendency of the model to reduce the incoming and existing water. Due to the values of T0 and T1, the amount of snow is more than rain, and therefore there is snow storage in the basin. The optimal value of α indicates that in the months when rain and snow are simultaneous, a small amount of precipitation is in the form of rain. The coefficients of hydraulic conductivity specify that the exchange between aquifers is less than expected. The level of the groundwater table shows that groundwater participation in surface runoff production has decreased and disappeared over time due to excessive abstraction of the aquifer and decreases in groundwater level. In addition, the optimized porosity values determined in the second scenario are more reasonable than the first one. The optimal values of surface runoff coefficients point to that the amount of available water to produce runoff is high, and the model tends to reduce the amount of outflow. The optimal values of the seasonal adjustment coefficients of evapotranspiration point to that the estimated ET are high, and the model has the tendency to reduce calculated ET. The values of initial moisture and maximum soil moisture capacity imply that it takes

time for soil moisture to reach its maximum capacity. The coefficient of surface runoff production designates that all the water in excess of soil moisture capacity infiltrates into the groundwater. The production coefficient of the base flow is not reasonable considering the threshold value of the groundwater level in order to participate in the production of streamflow. In both scenarios, the soil moisture reached its maximum value to produce surface and base flow in proportion to the observed values. In addition, the relationship between the water balance modules and the proposed mechanism for groundwater abstraction is such that the groundwater infiltration has occurred well in both models, which can be the reason for good fluctuations of groundwater level. Fig. 4 shows the times series and scatterplots of simulated/observed streamflow (at the watershed outlet) and groundwater level of the scenarios. However, the time series of the calculated streamflow has a weaker correlation with the observed values. In addition, the second scenario performs better in estimating the maximum values in most cases than the first ones. In addition, in the last years of the study period, streamflow has decreased, which can be happened because of increasing the cultivation area, reducing rainfall, and increasing water harvest. Given that there are no significant changes in the precipitation data and the cultivation area and harvesting recorded, it can be assumed that unauthorized groundwater abstraction has increased in recent years.

In the determinist water balance model (the first modelling scenario), the groundwater model is well-calibrated according to the statistical metrics. It happened because of the smaller number of parameters/variables affecting the groundwater balance model. In the first scenario, there was a requirement to provide median ET. This causes a large percentage of the available water to be used for ET. Therefore, less water remains to produce streamflow and infiltrate groundwater. The return water coefficient is equal to 0.28, indicating that a small amount of water is extracted from groundwater to meet the needs of agriculture to the existing water demand, which has reduced the production of surface water. Additionally, the values of SRC are close to the suggested upper limit of the parameter, which represents that the model has tried to produce more surface flow to improve the amount of the produced streamflow. Of course, this is due to the lower amount of water available due to the greater withdrawal of water from the available water to ensure ET. The coefficient of base flow generation in this scenario is low, which is a reason for the less consistency of the calculated groundwater fluctuations with the observed values. On the other hand, the amount of maximum soil moisture capacity (Smax) in this scenario is close to its upper limit, which indicates that the model tends to keep water in the soil to increase the available water, in which case it will have more water to provide ET.

The results of the second modelling scenario in a lower percentage of available water being used to provide ET. Therefore, more water remains to produce streamflow and infiltration. Given that in the second scenario, the ET is allowed to decrease to the minimum of the calculated ET, more water will be available to produce surface flow, which has led to better modeling of the outflow. As a result, penetration into the groundwater has also increased. Since the infiltration into the groundwater is a key parameter in producing groundwater fluctuations, this has led to an increase in the similarity values of aquifers. In the second scenario, the return water coefficient is more than the first scenario, which shows that more water extracted from groundwater has been added to the existing water to meet agricultural needs. This has increased the production of surface flow.

The proposed IBWB model, in addition to its advantages like the small size of the conceptual structures used in the monthly water balance, also has weaknesses in simulating streamflow. Since the time steps are monthly and assumed that the monthly rainfall is continuously and with very low intensity at a constant rate, the IBWB model simulates the streamflow less than it's actual. In addition, the approximate spatial interpolation in estimating rainfall over the study areas affects the simulation of the water balance model.

In uncertainty assessment, comparing the depicted histograms of the behavioral parameters and their posterior distributions in Table A4, the most important differences caused by the IBWB model on the parametric distributions could be inferred. Using the IBWB model (scenario 2), the coefficients required to moderate precipitation (PC) have a smaller posterior range than the first scenario. However, they have the same acceptable limits and asymmetric bell-shaped distributions. The coefficient α is logically in the range of [0, 1], which has led to a reduction in the frequency of selection of smaller coefficients than larger values in the second scenario model. In other words, the IBWB provides more precipitation values (versus snow) to circulate in the water balance model. As a result, the need for water storage to produce streamflow in warm seasons has been reduced. The logical range of returned flow (RF) is in the range of [0, 1], which has a case-specific range according to the characteristics of agriculture and irrigation network. In this research, higher values are more likely in the first scenario than in the second. It also seems that the model with ET adjustment coefficients (b) is generally based on lower values and both models behave the same in this regard. This range is the same for all seasons, and values close to 0 are more frequent.

In the first modeling scenario, the value of SRC has a semi-symmetric bell-shaped histogram with a median value of 0.62, close to its optimum value. In the histogram of the second scenario, this variable tends to have smaller values and is close to 0. The parameter has two different types of distributions in the scenarios.

Regarding the Smax values, in general, the selected range of the interval model was wider. This means that the soil is more likely to carry more moisture in this model due to the change in its structure. In addition, one of the important points is the considerable proximity of its median in all the studied plains with both methods (the range of 200 to 300 *mm*), which expresses the close behavior if the selection of a definite value will be necessary. In addition, the median values of the posterior distributions are significantly different from the optimal value, which can be considered as the effect of the equifinality assumption of the GLUE method. Moreover, both models tend to select higher porosity (η). Based on the local information, its maximum and minimum values have been set to 0.15 and 0.04, which according to previous reports of the Water Resources Management Company. The tendency to maximize porosity in practice means more water uptake (or release) with a slight change in soil moisture level. It also seems that the present model tends to increase this amount to manage excess surface water.

5. Conclusions

One of the most important concerns of water balance modeling is improving the estimation and uncertainties of various components that are used in the modeling procedure. Moreover, the ET model is one of the most important and complicated components with a vital role in this family of hydrological modeling. Typically, empirical relationships or physical models (e.g., Penman and Penman-Monteith models) have been used to estimate ET values. The

present study has been conducted to integrate modeling of watershed-scale ET based on the METRIC method with a comprehensive water balance model (combination of surface water and groundwater modules) in a developed basin. In addition, considering the parametric uncertainty and the various degrees of freedom in its initial conditions (such as hot/cold pixels), the model has a range of monthly ET values. As the first step to a paradigm shift from classic hydrologic model to hybrid the withe and gray ones, an Interval-Based Water Balance (IBWB) model has been developed to evaluate the uncertainty of the simulated ET using the METRIC model. Moreover, the median value was calculated as the definite answer and its corresponding interval as the uncertain answer. The case study is the Ghorveh-Dehgolan basin of the Sepidrood watershed, which is one of the developed agricultural areas with a considerable range of human interventions. Additionally, to compare the uncertainty behavior of the scenarios (classic and IBWB models) on the model parameters, the GLUE method has been used.

The results and statistical characteristics in the deterministic and non-deterministic conditions indicate the advantage of the proposed IBWB model over the deterministic modeling. The reduction of the uncertainty of the model's response as well as the improvement of the uncertainty performance metrics of the model are pieces of evidence of the improvement of the water balance model with an uncertain structure compared to the deterministic/classic ones. On the other hand, despite a fundamental change in the behavior and interaction of model components, especially the amount of evapotranspiration and groundwater abstraction, there was no significant change in the statistical behavior of model parameters. This means structural stability and appropriateness of probabilistic behavior and uncertainty of model parameters in the developed state compared to the classical structure. Based on the results, the improvement in decreasing the uncertainty of the groundwater levels is rich than the streamflow because of the considerable competency of the model in simulation of groundwater behavior.

Due to the importance of precipitation as the main and important driver of the water balance model and its uncertainty, it is suggested to develop a similar structure that can deliver uncertain behavior of precipitation in the structure of the deterministic water balance model. Overall, reviewing and developing the water balance model to use uncertain precipitation in the deterministic structure and combining it with the uncertain evapotranspiration is suggested as the next important step in this type of water balance modeling.

Declarations

Data Availability: The data that support the findings of this study are available from the corresponding author upon reasonable request.

Financial interests: All authors certify that they have no affiliations with or involvement in any organization or entity with any financial interest or non-financial interest in the subject matter or materials discussed in this manuscript.

References

1. Abedini MJ, Nasseri M (2008) Inverse distance weighted revisited. In *4th APHW, Conf. Beijing*
2. Ahmadi A, Nasseri M, Solomatine DP (2019) Parametric uncertainty assessment of hydrological models: coupling UNEEC-P and a fuzzy general regression neural network. Hydrol Sci J 64(9):1080–1094
3. Ahmadi A, Nasseri M (2020) Do direct and inverse uncertainty assessment methods present the same results? J Hydroinformatics 22(4):842–855
4. Al Zayed IS, Elagib NA, Ribbe L, Heinrich J (2016) Satellite-based evapotranspiration over Gezira Irrigation Scheme, Sudan: A comparative study. Agric Water Manage 177:66–76
5. Allen RG, Tasumi M, Trezza R (2007) Satellite-based energy balance for mapping evapotranspiration with internalized calibration (METRIC)—Model. J Irrig Drain Eng 133(4):380–394
6. Allen RG, Tasumi M, Morse A, Trezza R, Wright JL, Bastiaanssen W, Kramber W, Lorite I, Robison CW (2007) Satellite-based energy balance for mapping evapotranspiration with internalized calibration (METRIC)—Applications. J Irrig Drain Eng 133(4):395–406
7. Waters R, Allen R, Bastiaanssen W, Tasumi M, Trezza R (2002) Sebal. *Surface Energy Balance Algorithms for Land. Idaho Implementation. Advanced Training and User's Manual, Idaho, USA*
8. Baeumler NW, Kjaersgaard J, Gupta SC (2019) Evapotranspiration from corn, soybean, and prairie grasses using the METRIC model. Agron J 111(2):770–780
9. Bastiaanssen WG, Pelgrum H, Wang J, Ma Y, Moreno JF, Roerink GJ, Van der Wal T (1998) A remote sensing surface energy balance algorithm for land (SEBAL): Part 2: Validation. J Hydrol 212:213–229
10. Bastiaanssen WG, Menenti M, Feddes RA, Holtslag AAM (1998) A remote sensing surface energy balance algorithm for land (SEBAL). 1. Formulation. J Hydrol 212:198–212
11. Bastiaanssen WG (2000) SEBAL-based sensible and latent heat fluxes in the irrigated Gediz Basin, Turkey. J Hydrol 229(1–2):87–100
12. Bastiaanssen WG, Pelgrum H, Wang J, Ma Y, Moreno JF, Roerink GJ, Van der Wal T (1998) A remote sensing surface energy balance algorithm for land (SEBAL): Part 2: Validation. J Hydrol 212:213–229
13. Beven KJ, Binley A (1992) The future of distributed models, model calibration and uncertainty prediction. Hydrological Processe 6:279–298
14. Beven K, Binley A (2014) GLUE: 20 years on. Hydrol Process 28:5897–5918. 10.1002/hyp.10082 *doi*:
15. Çetin S, Köksal ES (2018) Potential use of remote sensing techniques in evapotranspiration estimations at watershed level. Environ Monit Assess 190(10):601
16. Chu W, Gao X, Sorooshian S (2011) A new evolutionary search strategy for global optimization of high-dimensional problems. Inf Sci 181(22):4909–4927

17. Corbari C, Ravazzani G, Mancini M (2011) A distributed thermodynamic model for energy and mass balance computation: FEST–EWB. Hydrol Process 25(9):1443–1452
18. Corbari CHIARA, Mancini MARCO, Li J, Su Z (2015) Can satellite land surface temperature data be used similarly to river discharge measurements for distributed hydrological model calibration. Hydrol Sci J 60(2):202–217
19. De Vos NJ, Rientjes THM, Gupta HV (2010) Diagnostic evaluation of conceptual rainfall–runoff models using temporal clustering. Hydrol Process 24(20):2840–2850
20. Duan Q, and Gupta. V (1992) Effective and Efficient Global Optimization Water Resources 28(4):1015–1031
21. Elkatoury A, Alazba AA, Mossad A (2020) Estimating Evapotranspiration Using Coupled Remote Sensing and Three SEB Models in an Arid Region. Environmental Processes 7(1):109–133
22. Guo S, Chen H, Zhang H, Xiong L, Liu P, Pang B, Wang G, Wang Y (2005) A semi-distributed monthly water balance model and its application in a climate change impact study in the middle and lower Yellow River basin. Water Int 30(2):250–260
23. Guo S, Wang J, Xiong L, Ying A, Li D (2002) A macro-scale and semi-distributed monthly water balance model to predict climate change impacts in China. J Hydrol 268(1–4):1–15
24. Gupta HV, Kling H, Yilmaz KK, Martinez GF (2009) Decomposition of the mean squared error and NSE performance criteria: Implications for improving hydrological modelling. J Hydrol 377(1–2):80–91
25. Herman MR, Nejadhashemi AP, Abouali M, Hernandez-Suarez JS, Daneshvar F, Zhang Z, Anderson MC, Sadeghi AM, Hain CR, Sharifi A (2018) Evaluating the role of evapotranspiration remote sensing data in improving hydrological modeling predictability. J Hydrol 556:39–49
26. Jazim AA (2006) A Monthly Six-parameter Water Balance Model and Its Application at Arid and Semiarid Low Yielding Catchments. Journal of King Saud University-Engineering Sciences 19(1):65–81
27. Jin X, Xu CY, Zhang Q, Singh VP (2010) Parameter and modeling uncertainty simulated by GLUE and a formal Bayesian method for a conceptual hydrological model. J Hydrol 30, 383((3–4):147–155
28. Jiang L, Wu H, Tao J, Kimball JS, Alfieri L, Chen X (2020) Satellite-Based Evapotranspiration in Hydrological Model Calibration. Remote Sensing 12(3):428
29. Kazumba S, Oron G, Honjo Y, Kamiya K (2008) Lumped model for regional groundwater flow analysis. J Hydrol 359(1–2):131–140
30. Knoben WJM, Freer JE, Woods RA (2019) Technical note: Inherent benchmark or not? Comparing Nash–Sutcliffe and Kling–Gupta efficiency scores. Hydrol Earth Syst Sci 23:4323–4331. https://doi.org/10.5194/hess-23-4323-2019
31. Kunnath-Poovakka A, Ryu D, Renzullo LJ, George B (2018) Remotely sensed ET for streamflow modelling in catchments with contrasting flow characteristics: an attempt to improve efficiency. Stoch Env Res Risk Assess 32(7):1973–1992
32. Losgedaragh SZ, Rahimzadegan M (2018) Evaluation of SEBS, SEBAL, and METRIC models in estimation of the evaporation from the freshwater lakes (Case study: Amirkabir dam. Iran) Journal of Hydrology 561:523–531
33. Lian J, Huang M (2016) Comparison of three remote sensing based models to estimate evapotranspiration in an oasis-desert region. Agric Water Manage 165:153–162
34. Lima JG, Sánchez JM, Piqueras JG, Espínola Sobrinho J, Viana PC, Alves ADS (2020) Evapotranspiration of sorghum from the energy balance by METRIC and STSEB. Revista Brasileira de Engenharia Agrícola e Ambiental 24(1):24–30
35. Lopez PL, Sutanudjaja EH, Schellekens J, Sterk G, Bierkens MF (2017) Calibration of a large-scale hydrological model using satellite-based soil moisture and evapotranspiration products. Hydrol Earth Syst Sci 21(6):3125–3144
36. Losgedaragh SZ, Rahimzadegan M (2018) Evaluation of SEBS, SEBAL, and METRIC models in estimation of the evaporation from the freshwater lakes (Case study: Amirkabir dam, Iran). J Hydrol 561:523–531. DOI:10.1016/j.jhydrol.2018.04.025
37. Liu W, Wang L, Zhou J, Li Y, Sun F, Fu G, Li X, Sang YF (2016) A worldwide evaluation of basin-scale evapotranspiration estimates against the water balance method. J Hydrol 538:82–95
38. Mirzaei M, Huang YF, El-Shafie A, Shatirah A (2015) Application of the generalized likelihood uncertainty estimation (GLUE) approach for assessing uncertainty in hydrological models: a review. Stoch Env Res Risk Assess 29(5):1265–1273
39. Murray SJ, Foster PN, Prentice IC (2012) Future global water resources with respect to climate change and water withdrawals as estimated by a dynamic global vegetation model. J Hydrol 448:14–29
40. Nash JE, Sutcliffe JV (1970) River flow forecasting through conceptual models part I—A discussion of principles. J Hydrol 10(3):282–290
41. Nasseri M, Zahraie B, Ansari A, Solomatin DP (2013) Uncertainty Assessment of Monthly Water Balance Models Based on Incremental Modified Fuzzy Extension Principle Method. J Hydroinformatics 15(4):1340–1360. DOI: 10.2166/hydro.2013.159
42. Nasseri M, Ansari A, Zahraie B (2014) Uncertainty Assessment of Hydrological Models with Fuzzy Extension Principle: Evaluation of a New Arithmetic Operator. Water Resour Res 50:1095–1111. DOI: 10.1002/2012WR013382
43. Nasseri M, Zahraie B, Poorsepahy-Samian H, Khodadadi M, Dolatabadi N (2021) Evaluation of Empirical Methods to Estimate Streamflow in Ungauged Basins (Case Study: The Sefidroud Watershed). Geography and Environmental Planning 32(1):1–24. doi: 10.22108/gep.2021.125717.1369
44. Nosrati K, Laaha G, Sharifnia SA, Rahimi M (2015) Regional low flow analysis in Sefidrood Drainage Basin, Iran using principal component regression. Hydrol Res 46(1):121–135
45. Rao AR, Al-Wagdany A (1995) Effects of Climatic Change in Wabash River Basin. J Irrig Drain Eng 121(2):207–215. doi: 10.1061/(asce)0733-9437(1995)121:2(207)

46. Reyes-González A, Kjaersgaard J, Trooien T, Hay C, Ahiablame L (2017) "Comparative Analysis of METRIC Model and Atmometer Methods for Estimating Actual Evapotranspiration", *International Journal of Agronomy*, vol. 2017, 16, 2017. https://doi.org/10.1155/2017/3632501
47. Schulz S, Becker R, Richard-Cerda JC, Usman M, Beek ausder, Merz T, Schüth C (2021) Estimating water balance components in irrigated agriculture using a combined approach of soil moisture and energy balance monitoring, and numerical modelling. *Hydrological Processes*, 35(3), p.e 14077
48. Schoups G, Nasseri M (2021) GRACE-Fully Closing the Water Balance: A Data-Driven Probabilistic Approach Applied to River Basins in Iran, *Water Resources Research*, 57, e2020WR029071. DOI: 10.1029/2020WR029071
49. Su Z (2002) The Surface Energy Balance System (SEBS) for estimation of turbulent heat fluxes. Hydrol Earth Syst Sci 6(1):85–100
50. Taghvaeian S, Neale CM (2011) Water balance of irrigated areas: a remote sensing approach. Hydrol Process 25(26):4132–4141
51. Taheri M, Emadzadeh M, Gholizadeh M, Tajrishi M, Ahmadi M, Moradi M (2019) Investigating the temporal and spatial variations of water consumption in Urmia Lake River Basin considering the climate and anthropogenic effects on the agriculture in the basin. Agric Water Manage 213:782–791
52. Taheri M, Gholizadeh M, Nasseri M, Zahraie B, Poorsepahy-Samian H, Espanmanesh V (2021) Performance evaluation of various evapotranspiration modeling scenarios based on METRIC method and climatic indexes. Environ Monit Assess 193(3):1–18
53. Thornthwaite CW, Mather JR (1957) Instructions and tables for computing potential evapotranspiration and the water balance. No. RESEARCH). Centerton
54. Shayeghi A, Azizian A, Brocca L (2020) Reliability of reanalysis and remotely sensed precipitation products for hydrological simulation over the Sefidrood River Basin, Iran. Hydrol Sci J 65(2):296–310
55. Solomatine DP, Shrestha DL (2009) A novel method to estimate model uncertainty using machine learning techniques.*Water Resources Research*, *45*(12)
56. Vervoort RW, Miechels SF, van Ogtrop FF, Guillaume JH (2014) Remotely sensed evapotranspiration to calibrate a lumped conceptual model: Pitfalls and opportunities. J Hydrol 519:3223–3236
57. Wani O, Beckers JVL, Weerts AH, Solomatine DP (2017) Residual uncertainty estimation using instance-based learning with applications to hydrologic forecasting. Hydrol Earth Syst Sci 21:4021–4036. https://doi.org/10.5194/hess-21-4021-2017
58. Waters R, Richard A, Tasumi M, Trezza R, Bastiaanssen W (2002) Surface Energy Balance Algorithms for Land, Advanced Training and User's Manual. A NASA EOSDIS/Synergy grant from the Raytheon Company through The Idaho Department of Water Resources
59. Xu CY, Seibert J, Halldin S (1996) Regional water balance modelling in the NOPEX area: development and application of monthly water balance models. J Hydrol 180(1–4):211–236
60. Yin J, Qiu X, Li S, Shi G, Liu H (2020) Estimation of evapotranspiration through an improved daily global solar radiation in SEBAL model: a case study of the middle Heihe River Basin.*Hydrology and Earth System Sciences Discussions*,1–32
61. Zhang Y, Chiew FH, Zhang L, Li H (2009) Use of remotely sensed actual evapotranspiration to improve rainfall–runoff modeling in Southeast Australia. J Hydrometeorol 10(4):969–980
62. Zhang K, Kimball JS, Running SW (2016) A review of remote sensing based actual evapotranspiration estimation. Wiley Interdisciplinary Reviews: Water 3(6):834–853
63. Yin Z, Liao W, Lei X, Wang H (2020) -Passing Interface Water 12(10):2667. http://dx.doi.org/10.3390/w12102667. Parallel Hydrological Model Parameter Uncertainty Analysis Based on Message
64. Xiang Y, Li L, Chen J, Xu C-Y, Xia J, Chen H, Liu J (2019) Parameter Uncertainty of a Snowmelt Runoff Model and Its Impact on Future Projections of Snowmelt Runoff in a Data-Scarce Deglaciating River Basin.*Water*,11
65. Smith KA, Barker LJ, Tanguy M, Parry S, Harrigan S, Legg TP, Prudhomme C, Hannaford J (2019) A multi-objective ensemble approach to hydrological modelling in the UK: An application to historic drought reconstruction. Hydrol Earth Syst Sci 23:3247–3268

Figures

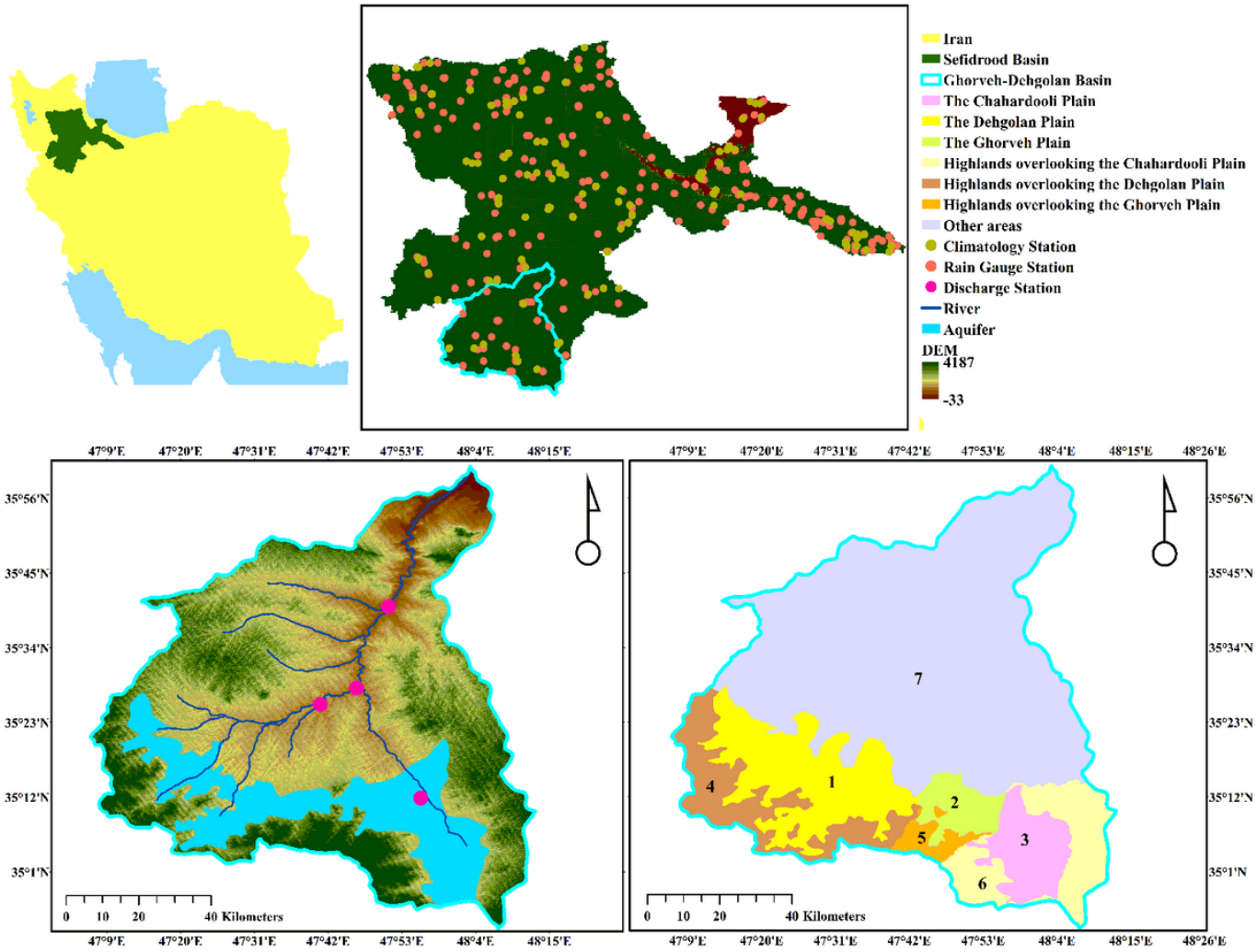

Figure 1

Location and DEM of Ghorveh-Dehgolan Basin, climatological and hydrometric network, Plain (areas 1, 2, and 3), HOLP (areas 4, 5, and 6) and OA (area 7)

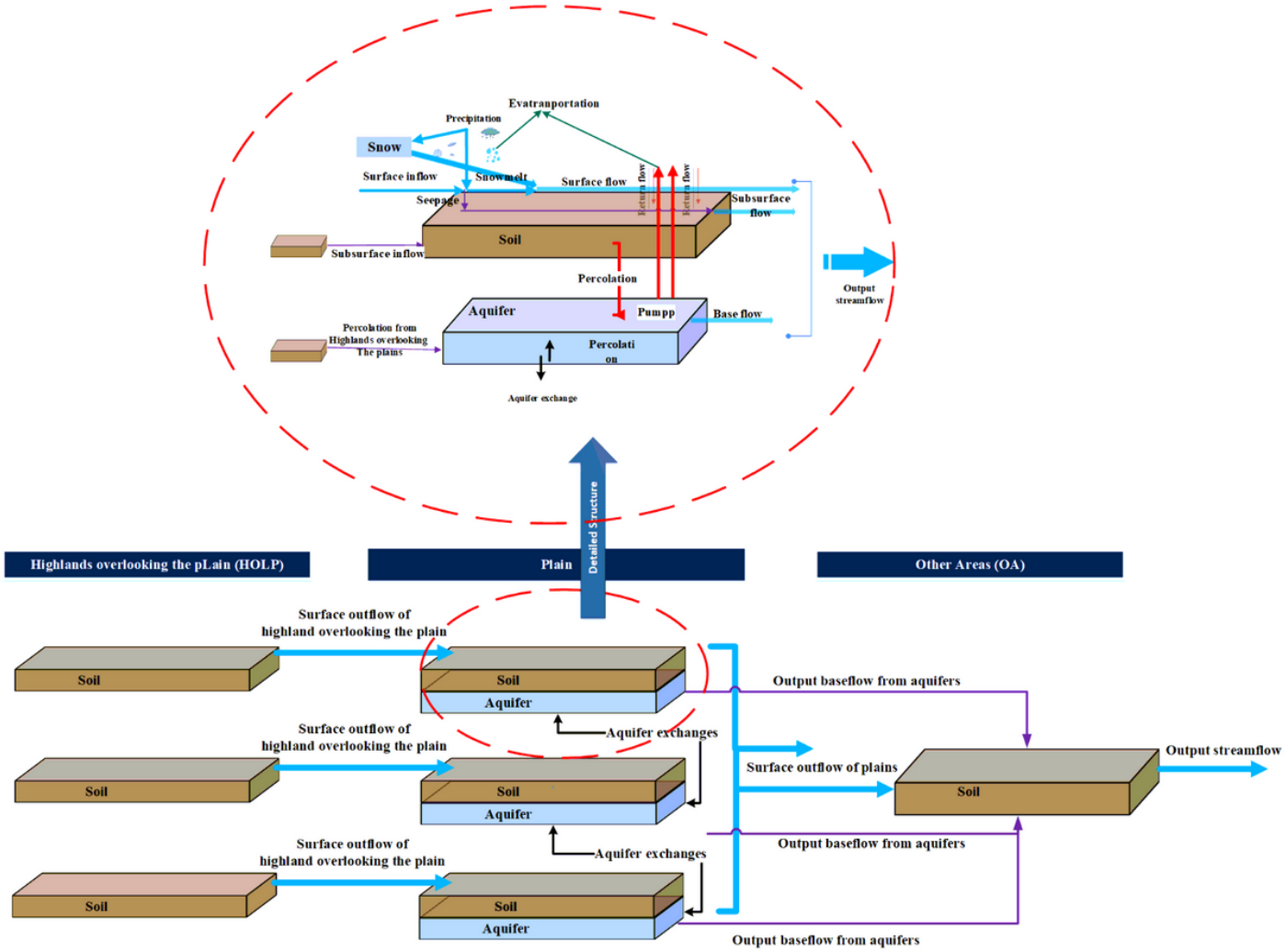

Figure 2

Interactions between different areas (Plains, HOLPs, and OA) of the basin in the used comprehensive water balance model

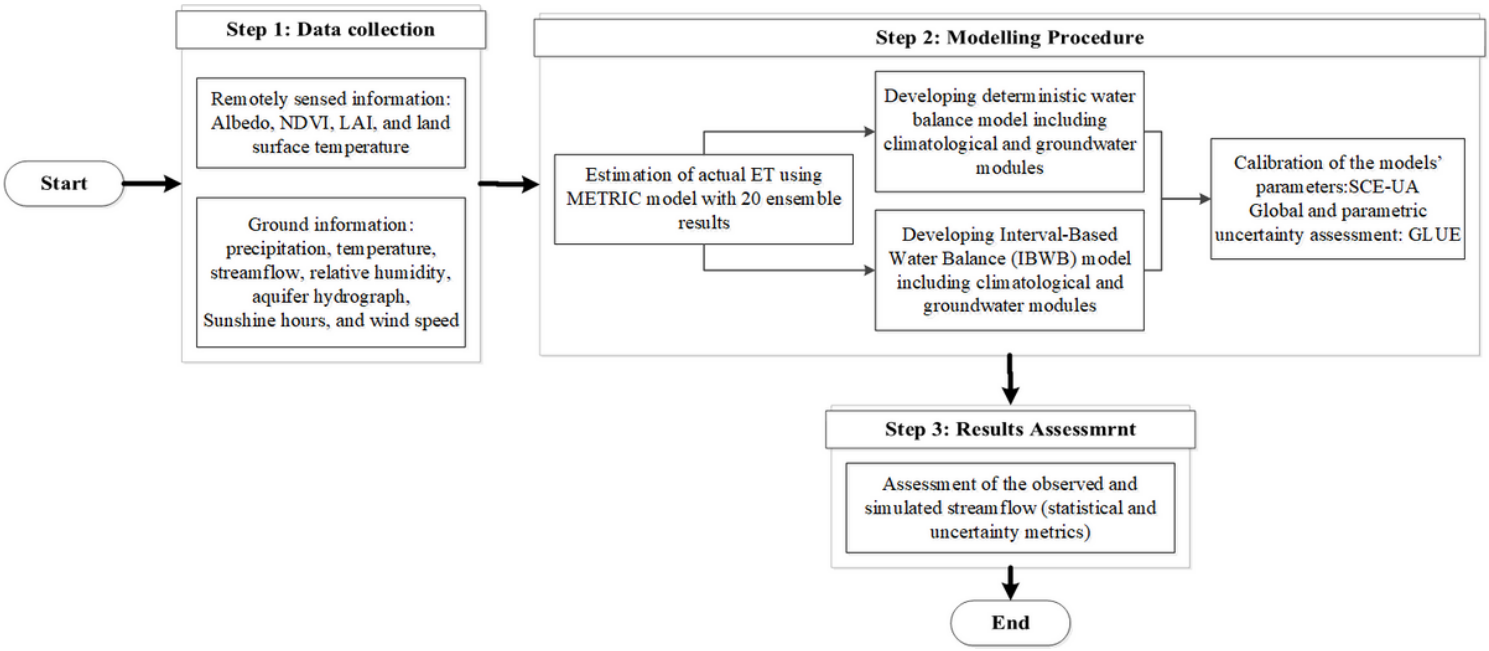

Figure 3

The flow diagram of the proposed methodology

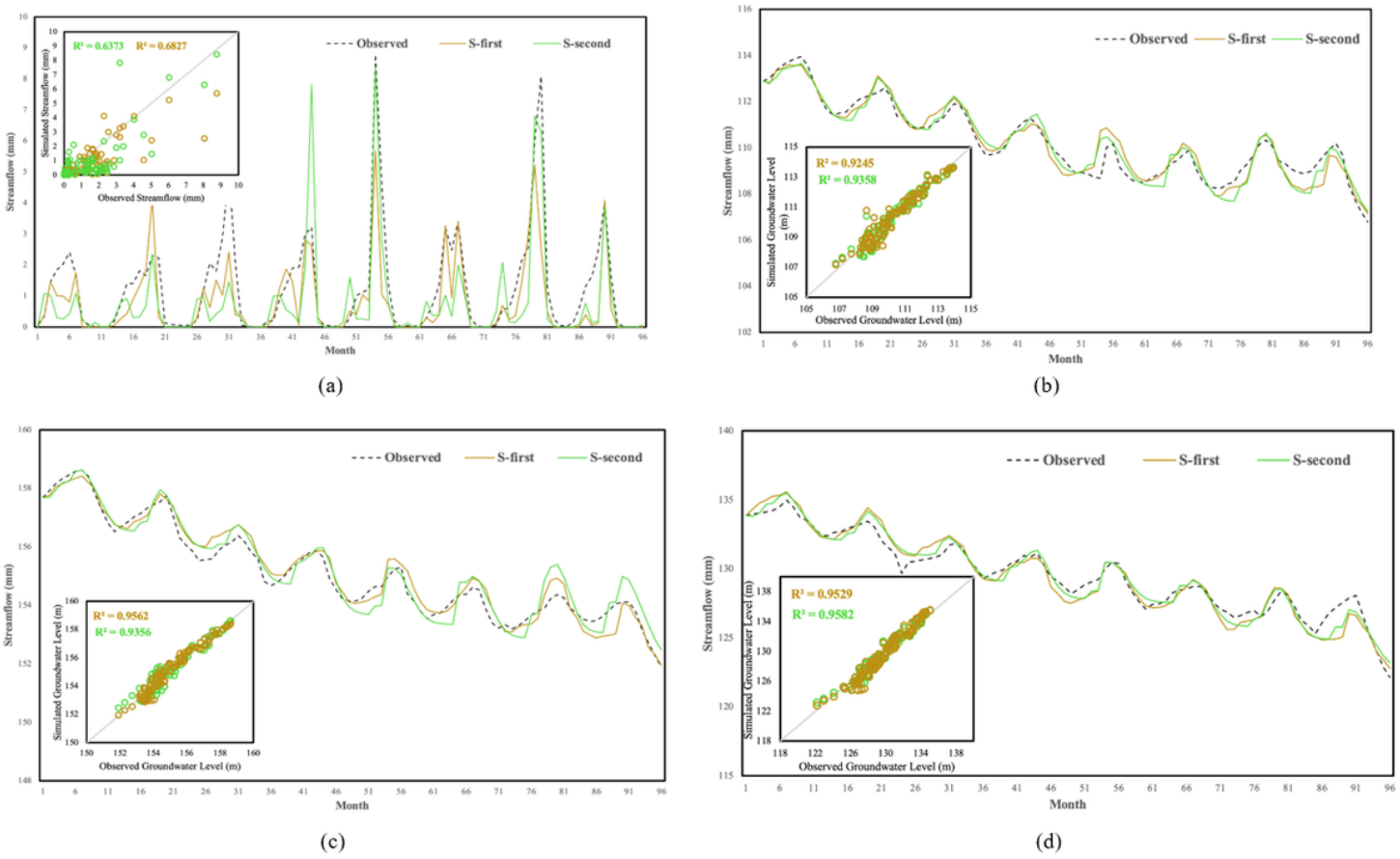

Figure 4

Time series and scatterplot of the a)observed and simulated streamflow in the outlet of the watershed (calibration period) b) groundwater level in Chardooli aquifer (calibration period) c) groundwater level in Gorveh aquifer (calibration period) d) groundwater level in Dehgolan aquifer (calibration period)

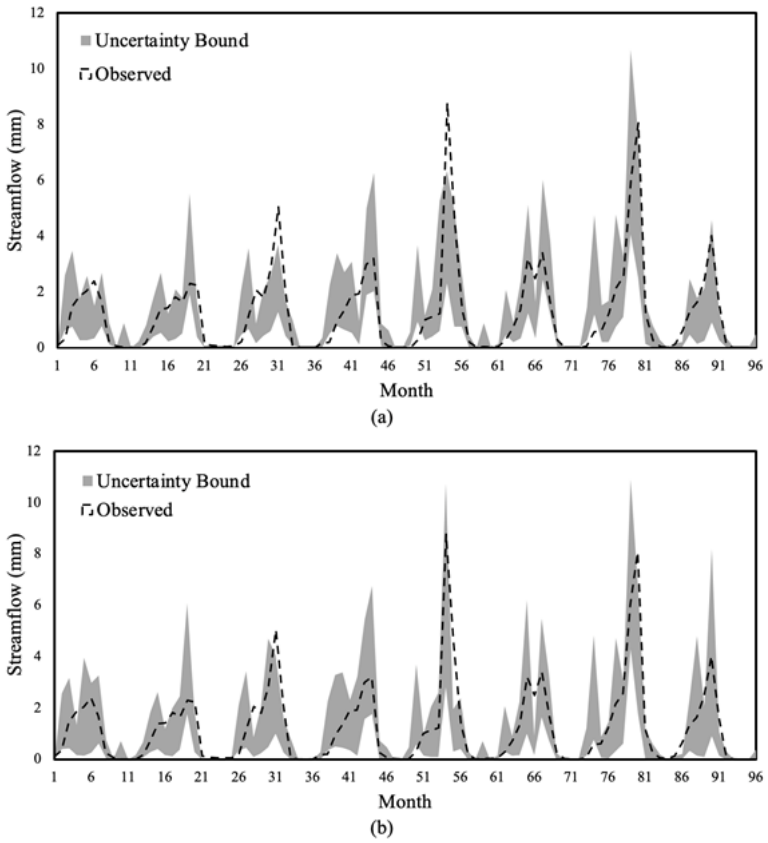

Figure 5

Observed and the simulated uncertainty bounds of the streamflow values for a) the first scenario and b) the second scenario

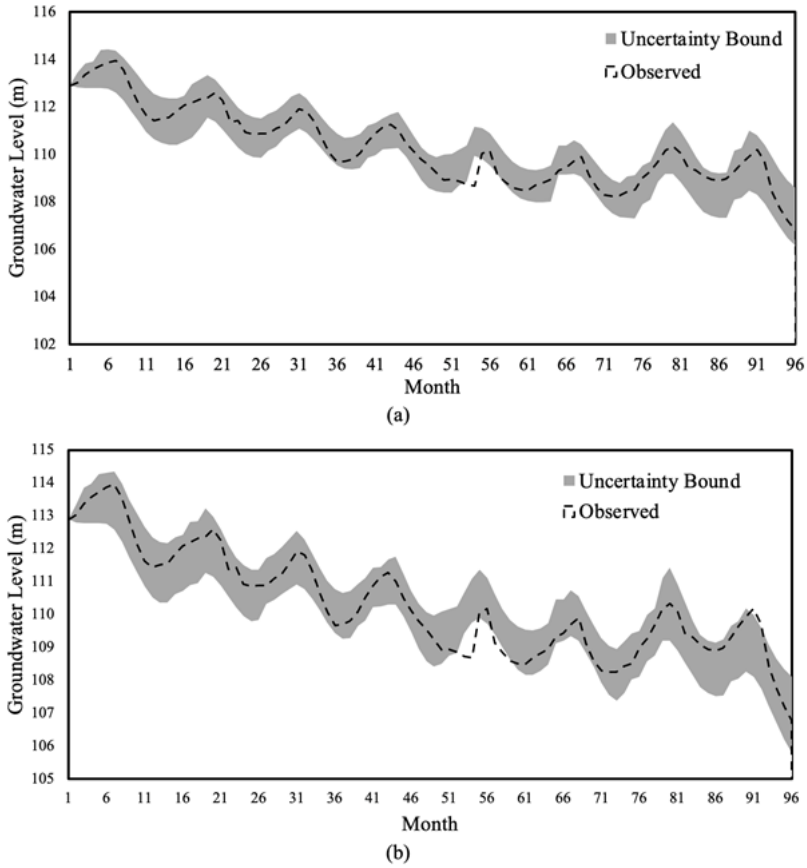

Figure 6

Observed and the simulated uncertainty bounds of the groundwater level in Chardooli aquifer values for a) the first scenario and b) the second scenario

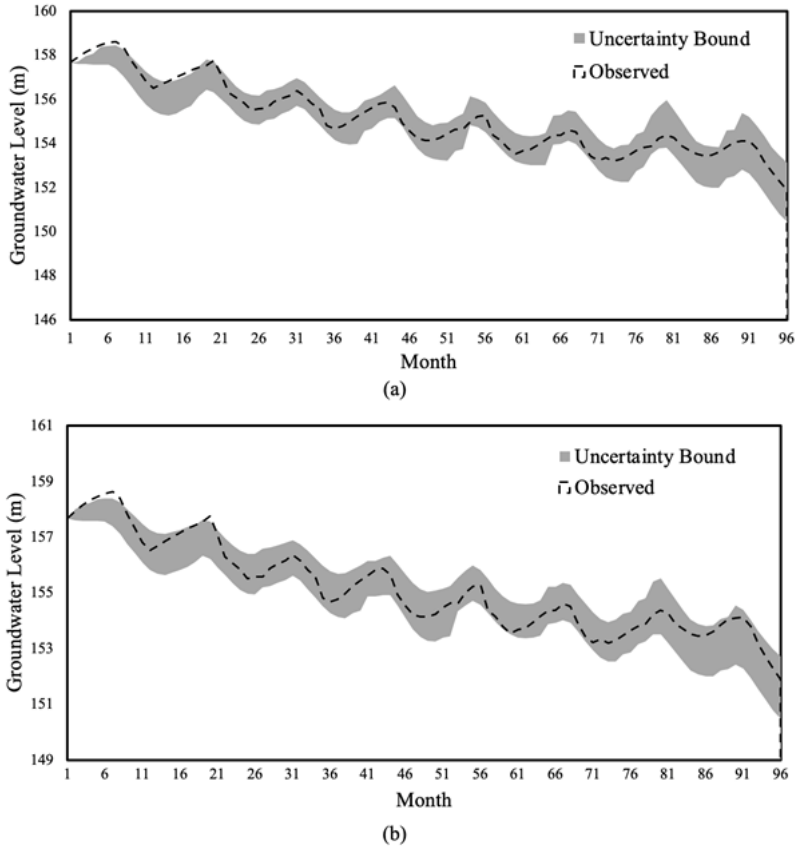

Figure 7

Observed and the simulated uncertainty bounds of the groundwater level in Gorveh aquifer values for a) the first scenario and b) the second scenario

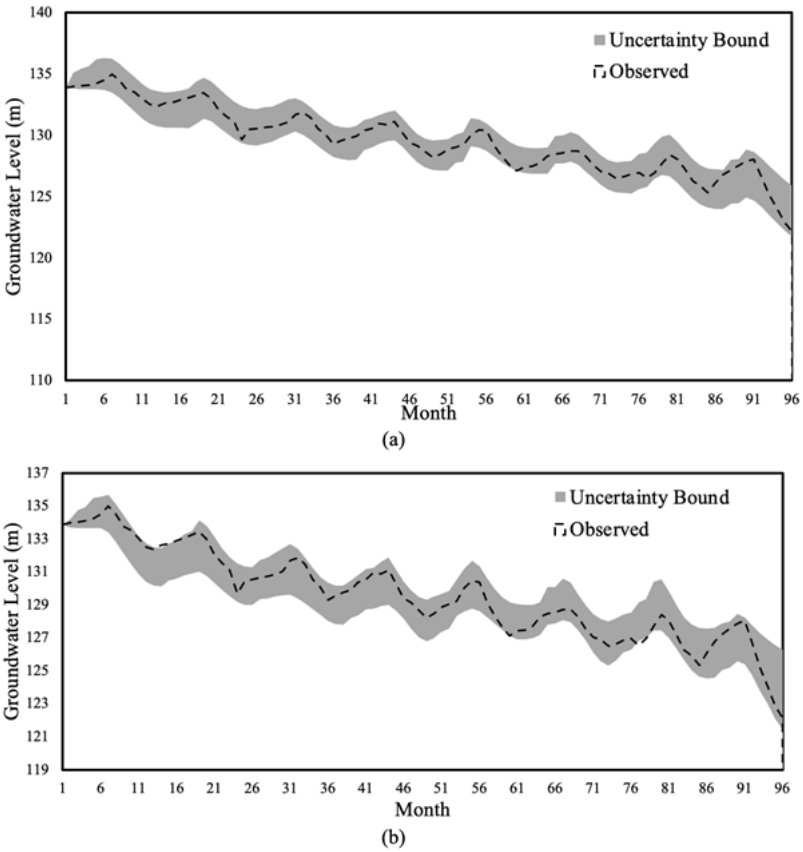

Figure 8

Observed and the simulated uncertainty bounds of the groundwater level in Dehgolan aquifer values for a) the first scenario and b) the second scenario

Supplementary Files

This is a list of supplementary files associated with this preprint. Click to download.

- Supp.docx